59. E. Maloney, D. Hartmann, *J. Clim.* **14**, 2015 (2001).
60. M. E. Mann, R. S. Bradley, M. K. Hughes, *Nature* **392**, 779 (1998).
61. ———, *Geophys. Res. Lett.* **26**, 759 (1999).
62. J. Esper, E. R. Cook, F. H. Schweingruber, *Science* **295**, 2250 (2002).
63. D. W. J. Thompson, S. Solomon, *Science* **296**, 895 (2002).
64. D. P. Schneider, E. J. Steig, *Geophys. Res. Lett.*, in press.
65. C. Appenzeller, T. F. Stocker, M. Anklin, *Science* **282**, 446 (1998).
66. J. Luterbacher *et al.*, *Geophys. Res. Lett.* **26**, 2745 (1999).
67. E. R. Cook, R. D'Arrigo, K. Briffa, *Holocene* **8**, 9 (1998).
68. L. Tremblay, L. A. Mysak, A. S. Dyke, *Geophys. Res. Lett.* **24**, 2027 (1997).
69. C. Schmutz *et al.*, *Geophys. Res. Lett.* **27**, 1135 (2000).
70. G. Bond *et al.*, *Science* **294**, 2130 (2001).
71. S. R. O'Brien *et al.*, *Science* **270**, 1962 (1995).
72. T. J. Crowley, *Quat. Res.* **21**, 105 (1984).
73. D. T. Shindell *et al.*, *Science* **294**, 2149 (2001).
74. P. M. Grootes *et al.*, *Nature* **366**, 552 (1993).
75. J. P. Sachs, S. J. Lehman, *Science* **286**, 756 (1999).
76. L. Stott, C. Poulsen, S. Lund, R. Thunell, *Science* **297**, 222 (2002).
77. A. Koutavas, J. Lynch-Stieglitz, T. M. Marchitto Jr., J. P. Sachs, *Science* **297**, 226 (2002).
78. W. S. Broecker, *Science* **278**, 1582 (1997).
79. C. D. Charles, R. G. Fairbanks, *Nature* **355**, 416 (1992).
80. J. F. Adkins *et al.*, *Science* **280**, 725 (1998).
81. L. D. Keigwin, E. A. Boyle, *Proc. Natl. Acad. Sci. U.S.A.* **97**, 1343 (2000).
82. G. A. Meehl, J. M. Arblaster, W. G. Strand Jr., *Clim. Dyn.* **16**, 257 (2000).
83. D. Rind, R. Healy, C. Parkinson, D. Martinson, *J. Clim.* **8**, 449 (1995).
84. ———, *Geophys. Res. Lett.* **24**, 1491 (1997).
85. M. M. Holland, C. M. Bitz, in preparation.
86. P. D. Jones, *J. Clim.* **7**, 1794 (1994).
87. E. Kalnay *et al.*, *Bull. Am. Meteorol. Soc.* **77**, 437 (1996).
88. G. A. Meehl, G. J. Boer, C. Covey, M. Latif, R. J. Stouffer, *Bull. Am. Meteorol. Soc.* **81**, 313 (2000).
89. We thank J. Walsh, D. Hartmann, G. Roe, J. Morison, and one anonymous reviewer for helpful comments. This research was supported by the NSF through grant OPP0084287.

REVIEW

Mass Balance of Polar Ice Sheets

Eric Rignot[1] and Robert H. Thomas[2]

Recent advances in the determination of the mass balance of polar ice sheets show that the Greenland Ice Sheet is losing mass by near-coastal thinning, and that the West Antarctic Ice Sheet, with thickening in the west and thinning in the north, is probably thinning overall. The mass imbalance of the East Antarctic Ice Sheet is likely to be small, but even its sign cannot yet be determined. Large sectors of ice in southeast Greenland, the Amundsen Sea Embayment of West Antarctica, and the Antarctic Peninsula are changing quite rapidly as a result of processes not yet understood.

The Antarctic and Greenland ice sheets together hold 33 million cubic km of ice, representing enough water to raise global sea level by 70 m. Annual snowfall on the ice sheets is equivalent to 6.5 mm of sea level, so that only a small imbalance between snowfall and discharge of ice and meltwater into the ocean could be a major contributor to present-day sea-level rise [~1.8 mm/year (*1*)]. Large variations in sea level over the past million years have in fact been controlled by ice, with rates of sea-level rise at least one order of magnitude larger than at present during times of rapid deglaciation. Consequently, a detailed knowledge and understanding of the evolution of polar ice sheets is of considerable societal importance, and here we review current progress based on observations made during the last decade.

The balance between net accumulation and attrition of ice is not the same for the two ice sheets, owing to differences in climatic regime. Antarctica has a dominant influence on its own climate and on the surrounding ocean, with cold conditions even during the summer and around its northern margins, so there is little surface melting, even near the coast. Vast floating ice shelves exist around much of the periphery of the continent, fed in part by ice discharged from the ice sheet by outlet glaciers and ice streams, some penetrating deep into the heart of Antarctica. Ice is lost primarily by basal melting and iceberg calving from these ice shelves.

By contrast, Greenland's climate is strongly affected by nearby land masses and the North Atlantic, with the Gulf Stream to the south. The average accumulation rate (~30 cm/year) is twice that for Antarctica. Summer melting occurs over half of the ice-sheet surface, with much of the water flowing to the sea. The ice sheet is fringed almost completely by coastal mountains through which it is drained by many glaciers. Ice is lost primarily by surface runoff and iceberg calving, except in the north where basal melting from small ice shelves is substantial.

These ice sheets were much larger at the last glacial maximum, some 21,000 years ago, retreating to their present condition in the last few thousand years. Their present mass balance depends on this long-term trend, determined by past climate and dynamic history, and on more recent changes in climate and ice-sheet dynamics. A major challenge of modern glaciology is to separate the long-term background signal from more recent changes.

Ice-Sheet Mass Balance

There are three ways to measure the mass balance of an ice sheet:

(i) The mass budget method, which compares losses by melting and ice discharge with total net input from snow accumulation. Net accumulation is inferred primarily from ice-core measurements, with 5% errors for large-area averages (*2*–*4*). Loss by melting is more complex because of meltwater refreezing after draining into near-surface snow (*5*). Melt rates are commonly estimated from positive degree-day models (*6*). Although large uncertainties suggest that accurate mass-balance determination for an entire ice sheet is difficult by the mass budget method, it can be achieved for smaller regions by measuring ice discharge inland of the grounding line, an approach made possible by new techniques for measuring ice velocities over large areas from Global Positioning System (GPS) and interferometric synthetic-aperture radar (InSAR) data, provided that ice thickness is known.

(ii) Measurements of elevation change over time, which are translated into measurements of volume change by including estimates of the vertical motion of underlying ground associated with isostatic rebound or tectonics. Satellite radar altimeters (Seasat, Geosat, and European Remote Sensing Satellites ERS-1 and -2) have been used to infer elevation change rates over Greenland and Antarctica since 1978 (*7*, *8*). Coverage is limited to the interior regions of the ice sheets, where surface slopes are low. Aircraft altimeters were used extensively over Greenland in the 1990s (*9*). Launch of NASA's Ice, Cloud, and Land Elevation Satellite (ICESat), with a laser altimeter and orbit coverage to 86°S, and the European Cryosat, with a small-footprint radar altimeter extending to 88°S, will increase measurement accuracy and extend surveys to the interior regions and to the ice-sheet margins, where remote sensing measurements are most challenging and thickness changes are most pronounced.

(iii) Weighing of the ice sheets. NASA's

[1]Jet Propulsion Laboratory, California Institute of Technology, Mail Stop 300-235, Pasadena, CA 91109, USA. [2]EG&G Services, Wallops Flight Facility, Building N-159, Wallops Island, VA 23337, USA. E-mail: eric@adelie.jpl.nasa.gov, robert_thomas@hotmail.com

Gravity Recovery and Climate Experiment (GRACE) satellite mission will provide gravity-change measurements, which, combined with ICESat data, could yield estimates of the mass balance of the Antarctic Ice Sheet equivalent to a sea-level change of 0.2 mm/year, and may enable the separation of the long-term viscous response of the crust from its present-day elastic response (*10, 11*).

Each method addresses a complementary aspect of the determination of ice-sheet mass balance. This review concentrates on new results from the first two methods.

Greenland

During the 1990s, a series of measurements by NASA's Program for Arctic Regional Climate Assessment showed higher elevation parts of the ice sheet to be broadly in balance, with appreciable thinning nearer the coast (*12*). Although the higher elevation region taken as a whole is in balance to within 1 cm/year thickening/thinning rate, smaller areas within the region are thickening or thinning at rates up to 30 cm/year, primarily because of temporal variability in snow-accumulation rates (*13*). These results are based on repeated airborne laser altimeter and satellite radar altimeter surveys (*7, 9, 14*) and on the mass budget method applied to the region above ~2000 m elevation (*15*) and to individual glacier catchment basins (*16, 17*) (Fig. 1).

In contrast to overall balance at higher elevations, the coastal regions thinned rapidly between the 1993–94 and 1998–99 aircraft laser altimeter surveys, with thinning concentrated along channels occupied by the outlet glaciers. A conservative ice loss estimate of 50 km^3/year was inferred from the survey, sufficient to raise sea level by 0.13 mm/year (*9*). The rapid thinning of many outlet glaciers (up to several meters per year) is greater than can be explained by increased melting associated with recently warm summers (*14*) after a cool period in the 1970s and 1980s (*18*). Consequently, the observed coastal thinning appears to represent dynamic glacier behavior rather than an ephemeral surface response to atmospheric warming.

Glacier thinning is most pronounced in the southeast but also predominates in the northwest. Both quadrants of the ice sheet further inland also show thinning over the past few decades, as indicated by the mass budget analysis (*15*) and comparison with surveys conducted in the 1950s (*19*). The average rate of thinning in the southeast sector is 30 cm/year over an area of 34,000 km^2 between the 2000-m contour and the northsouth ridge. Snow accumulation rates are the highest in Greenland, and outlet glaciers are very active, poorly documented, but likely to accommodate a rapid mass turnover.

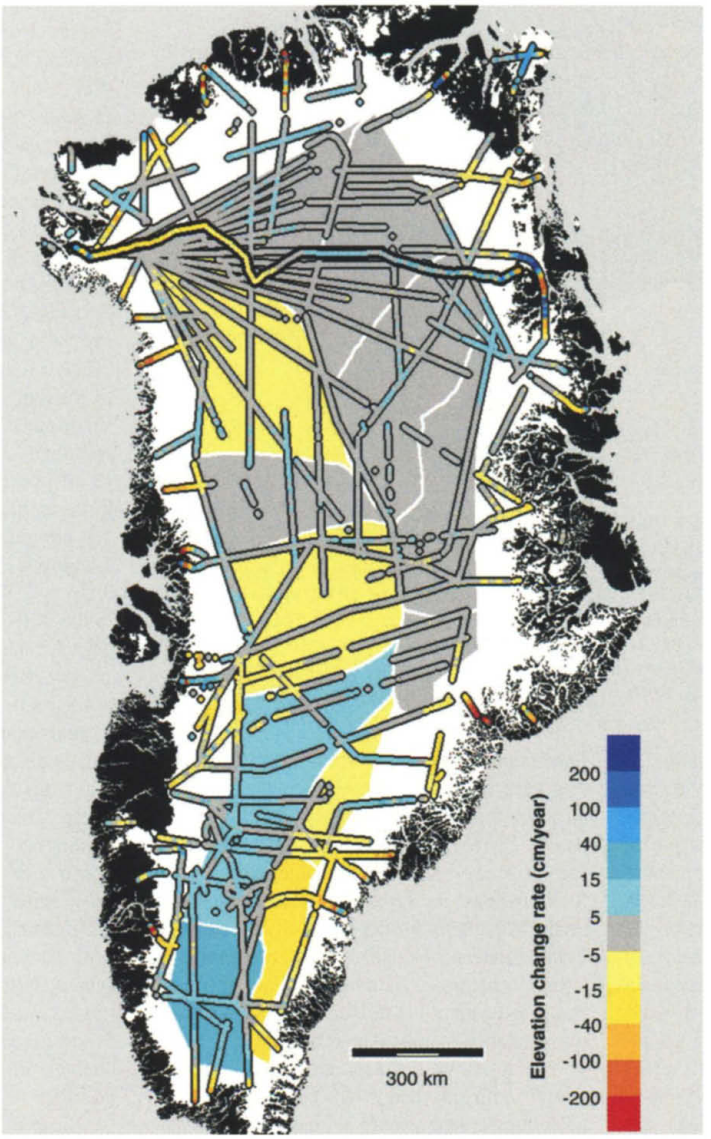

Fig. 1. Estimated ice thickening rates in Greenland, based on mass budget calculations (*15*) and direct measurement of changes in surface elevation (*9, 19*). The mass budget estimates for each studied sector are color-coded. Estimates from elevation changes are color-coded along laser flight lines (narrow) and along a surveyed traverse in the north (broad). The laser estimates refer to 1993–94 to 1998–99, the surveyed traverse to 1954–1995, and the mass budget to approximately 1970–1995.

Most Greenland glaciers are tidewater glaciers flowing directly into the ocean with little or no floating section, but in the north, slowly moving colder glaciers flow into ice shelves. Earlier mass-balance studies found a largely positive mass budget for these glaciers, due to low iceberg discharge, but this becomes negative when pronounced melting from beneath the ice shelves is fully taken into account (*16*). Although the melting of floating sections does not raise sea level, the high rates of bottom melting inferred for the floating sections imply that a small increase in thermal forcing from the ocean could rapidly initiate their demise, which may in turn allow more rapid discharge from the outlet glaciers and more negative mass balance for the ice sheet. Several observations suggest large recent changes in both the North Atlantic and the Arctic (*20, 21*), which may have increased bottom melt rates.

But this does not explain the simultaneous thinning of almost all surveyed glaciers, with and without ice shelves. One possibility is increased basal lubrication associated with the availability of additional surface meltwater reaching the glacier bed via crevasses and moulins (*22*). This plausible mechanism for rapid, wide-scale dynamic response to atmospheric warming would imply even greater thinning during the very warm period in the 1930s to 1960s (*18*), which might indeed explain the widespread marginal retreat in southern Greenland ending in the 1950s, inferred from historical records (*23*).

Antarctica

Recent advances in our understanding of the mass balance of the Greenland Ice Sheet were made possible by technical advances in remote sensing (particularly laser altimetry, radar altimetry, InSAR, and GPS), comparative ease of access and logistics, geographical location within satellite coverage, and small ice-sheet area. Antarctica is a harder nut to crack because it is far larger, more remote, and not well covered by existing key satellites. Consequently, accurate mass budget estimates have been made for limited regions, and elevation changes have been directly measured only for gently sloping parts of the ice sheet north of 81.5°S.

Using few estimates of ice flux through

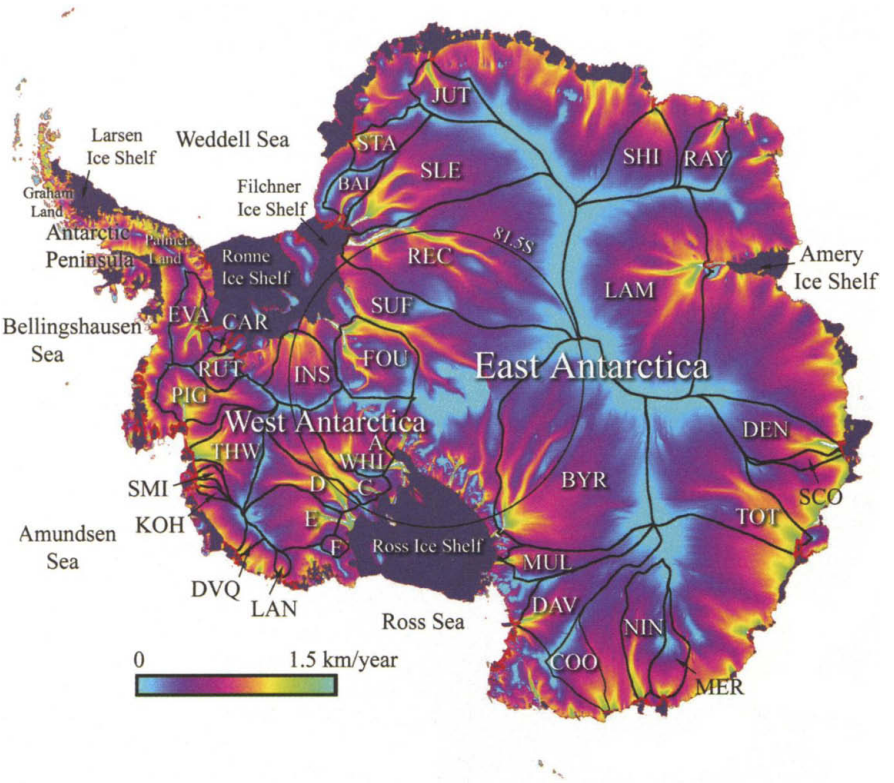

Fig. 2. Location of 33 Antarctic glaciers (Table 1) overlaid on a map of calculated ice-sheet balance velocity (*54*). Catchment basin boundaries are black, grounding lines are red, and ice shelves are gray. Abbreviations for glaciers: Pine Island (PIG), Thwaites (THW), Smith (SMI), Kohler (KOH), DeVicq (DVQ), Land (LAN), Whillans (WHI), A-F (A-F), Byrd (BYR), Mulock (MUL), David (DAV), feeding eastern Cook Ice Shelf (COO), Ninnis (NIN), Mertz (MER), Totten (TOT), Denman (DEN), Scott (SCO), Lambert/Mellor/Fisher (LAM), Rayner (RAY), Shirase (SHI), Jutulstraumen (JUT), Stancomb-Wills (STA), Bailey (BAI), Slessor (SLE), Recovery (REC), Support-Force (SUF), Foundation (FOU), Institute (INS), Rutford (RUT), Carlson (CAR), and Evans (EVA).

gates near the margin and snow accumulation, a positive mass budget of 42 to 436 km^3/year had earlier been estimated for Antarctica, suggesting that Antarctica was not contributing to sea-level rise (*24*). Improved estimates of snow accumulation rates (*3, 4*), a digital elevation model of Antarctica (*25*), a compilation of thickness data (*26*), and a radar mosaic (*27*) have since been published. InSAR has been used to measure glacier velocities (*28–30*) and to map grounding-line positions (where ice detaches from the bed and becomes afloat), often found to be tens of km away from previously assumed positions (Fig. 2). Ice thickness, the least well-constrained mass budget parameter, is inferred primarily from hydrostatic equilibrium near the grounding line.

This work indicates substantial losses or balance for large areas such as Pine Island, Thwaites, Lambert, Totten, and Jutulstraumen glaciers (Table 1) previously thought to be gaining mass (*24*), and large gains for the Ross ice streams in West Antarctica (*31*) previously thought to have been losing mass (*32*). The 12 surveyed East Antarctic glaciers not draining into a major ice shelf, and the eight glaciers draining into the Filchner/Ronner Ice Shelves, appear to be close to balance (Table 1). Large uncertainties remain for areas south of 81.5°S (e.g., Byrd Glacier), forcing reliance on old airborne topographic surveys where ice thickness is poorly known, and InSAR coverage is incomplete. No satellite coverage exists for the Support-Force ice stream and several Transantarctic Mountains glaciers. The divide between Foundation and Support-Force ice streams is poorly constrained by available data (*4*). As a result, we cannot yet reliably estimate ice-sheet mass balance in East Antarctica.

Much of West Antarctica is a "marine ice sheet" with its bed well below sea level, prompting concerns over its stability in a warming climate (*33*). This region has received more attention over the past 20 years, particularly the Siple Coast ice streams flowing into the Ross Ice Shelf (*34*). These ice streams are unusual in that they have low surface slopes and therefore low forces driving their motion seaward. This is possible because their beds are lubricated by muddy sediments (*35*), but it means that quite small changes in the distribution and thermal state of basal water can have large impacts on ice velocity. Indeed, the main reason for the positive balance of this region is the stoppage of ice stream C about 150 years ago and the ongoing slowing of Whillans ice stream (*31*).

In contrast, the sector draining West Antarctica into the Amundsen Sea Embayment (ASE) has a negative imbalance of double this rate, as judged by mass budget estimates (*36–38*), elevation changes (*8, 39, 40*), and measured grounding-line retreat (*36*). In contrast to Whillans' deceleration rate of 5 m year^{-2}, Pine Island Glacier is accelerating by 45 m year^{-2} and Thwaites Glacier is widening by several kilometers per year (*38*). The rapid evolution of ice in this sector is not limited to these two large glaciers: Smith, Kohler, DeVicq, and Land glaciers contribute even more to the negative imbalance (Table 1), and Smith Glacier is thinning twice as rapidly as Thwaites Glacier (*41*).

The inferred ice loss of 72 ± 12 km^3/year from the sector between Pine Island and Land glaciers (Table 1) is consistent with an ice loss of 67 ± 13 km^3/year estimated from radar altimetry between Pine Island and Kohler glaciers (*39*). Overall, the West Antarctic Ice Sheet appears to be losing at least 48 ± 14 km^3/year (Table 1, which excludes sectors north of Evans/Pine Island and between Kohler, DeVicq, and Land glaciers that are thinning according to radar altimetry) and as much as 76 ± 15 km^3/year [(*39*), which excludes Foundation, Institute, half of C, and A/Whillans ice streams that are gaining 11 km^3/year in Table 1]. This total loss is sufficient to raise sea level by about 0.16 ± 0.05 mm/year. Continued acceleration in the ASE could lead to a substantially more negative mass balance.

The ice shelves in the ASE have very high basal melt rates, in the range of 10 to 40 m/year near the grounding line (*42*). These values are consistent with high thermal forcing from the ocean caused by intrusion of warm Circumpolar Deep Water across the continental shelf. Progressively warmer ocean conditions are suggested by recent data (*43*), with an associated increase in basal meltwater production of 50 km^3/year in recent decades. Rapid ice-shelf thinning observed with radar altimetry (*39*)—up to 4 m/year on the ice shelves fed by Kohler and Smith glaciers (Fig. 2)—confirms that the ice shelves in the ASE are changing rapidly, possibly in reaction to a warmer ocean.

Little is known about the mass balance of the mountain glaciers in the Antarctic Peninsula, which, although representing only 7% of Antarctica's area, receives a quarter of its accumulation and holds enough ice to raise sea level by a third of a meter (*44*). These glaciers are distinct from most others in Antarctica; they are much smaller and are subject to different climate conditions, including extensive surface melting in the summer. The peninsula's proximity to the ocean and low latitude make it the most likely part of Antarctica to show signs of climate change (*33*). Indeed, the Antarctic Peninsula has experienced a vigorous regional warming of 2° to

3°C in the last 50 years (*45*), with associated thinning, enhanced melting, and rapid disintegration of its ice shelves (*46, 47*). Although the collapse of floating ice shelves has no effect on sea level, it could have a profound influence on ocean circulation, climate, and the dynamics of tributary glaciers.

On the basis of observational evidence (*48–50*) and theory (*51*), it has been argued that ice-shelf retreat has little effect on glaciers that flow into ice shelves, refuting earlier suggestions that the removal of ice shelves would allow faster rates of ice discharge along those glaciers (*52*). The rapid loss of ice shelves from the Antarctic Peninsula provides an opportunity to test these predictions. In western Palmer Land, no ice-flow changes were observed after the demise of the Wordie Ice Shelf (*48*), but in eastern Graham Land, in the 4 years since the breakup of parts of the Larsen Ice Shelf, tributary glaciers accelerated by as much as a factor of 3 (*53*). These modern observations shed new light on the possibility of eustatic sea-level change caused by ice-shelf retreat, whether caused by regional atmospheric warming in the Antarctic Peninsula or possibly by ocean warming in the ASE. If the ice shelves do buttress their tributary glaciers and substantially modulate their flow, sea-level change in a warming climate could be far greater than currently predicted for Antarctica.

The Future

Although the past two decades have seen major advances in our characterization of large areas of Greenland and Antarctica, primarily because of the widespread application of remote-sensing techniques, it is still not possible to determine even the sign of ice-sheet mass balance in East Antarctica until new data are collected. West Antarctica exhibits a bimodal behavior, with thickening in the west and more rapid thinning to the north, but is probably losing mass overall at a rate sufficient to raise sea level by almost 0.2 mm/year. The Greenland Ice Sheet is losing mass at a rate sufficient to raise sea level by at least 0.13 mm/year because of rapid near-coastal thinning. Appropriate observations must be continued to determine whether this is part of a long-term trend. The upcoming ICESat and Cryosat satellite missions, in combination with GRACE, will yield mass-balance estimates for all of Greenland and most of Antarctica and will include coverage of more steeply sloping coastal regions. Understanding of these observations, however, will require widespread InSAR and ice thickness surveys complemented by targeted in situ measurements.

Perhaps the most important finding of the past 20 years has been the rapidity with which substantial changes can occur on polar ice sheets. As measurements become more precise and more widespread, it is becoming increasingly apparent that change on relatively short time scales is commonplace: stoppage of huge glaciers, acceleration of others, appreciable thickening and far more rapid thinning of large sectors of ice sheet, rapid breakup of vast areas of ice shelf and acceleration of tributary glaciers, surface melt-induced acceleration of ice-sheet flow, and vigorous bottom melting near grounding lines. These observations run counter to much of the accepted wisdom regarding ice sheets, which, lacking modern observational capabilities, was largely based on "steady-state" assumptions. Of particular importance, in light of recent warming in the Antarctic Peninsula and the progressive demise of its ice shelves, is to determine how this will affect glacier discharge rates and sea-level rise, with obvious implications for predicting the evolution of larger sectors of the Antarctic Ice Sheet.

Table 1. Mass budget of 33 Antarctic glaciers that include 25 of the 30 largest ice producers. In each row, snow accumulation (*3*) minus grounding-line outflow [(*30, 31, 38, 42*), except FOU, BAI, RAY, COO, and MUL from this study] yields net balance. The uncertainty in accumulation is assumed to be 5%, which may be an underestimate. Accumulation values in parentheses (*4*) are not used to calculate net balance; they seem to overestimate accumulation in East Antarctica, possibly because of a more computerized interpolation of the data. In regions where the two accumulation numbers differ most (e.g., BYR, DEN, TOT, DAV), the uncertainty in accumulation is likely to be higher than 5%. The uncertainty in outflow is dominated by uncertainties of 100 m in ice thickness derived from hydrostatic equilibrium, and of a few tens of meters from radio echo sounding data (PIG, A/WHI, B-F) (*26, 31*). Ice thickness deduced from hydrostatic equilibrium uses surface elevation near the grounding line and a conversion factor taking account of different seawater and ice densities. Grounding-line positions are from InSAR, except those of INS, REC, RAY, MUL, and BYR, which are from hydrostatic equilibrium. Ice velocity measurements for A/WHI, C-F, INS, FOU, BAI, SLE, REC, COO, LAM, RAY, STA, BYR, and MUL are from Radarsat-1; for other glaciers, tandem measurements from ERS-1 and -2 are shown (PIG/THW data collected in 2000).

Glacier	Area (km^2)	Accumulation (km^3/year)	Outflow (km^3/year)	Net (km^3/year)
PIG	162,300	74.2 (70.5)	82.6 ± 4	−8
THW	164,800	57.6 (61.3)	80.1 ± 8	−23
SMI	16,500	6.5 (5.9)	19.3 ± 2	−13
KOH	10,200	2.7 (3.0)	9.9 ± 1	−7
DVQ	16,000	4.7 (4.9)	18.8 ± 2	−14
LAN	12,800	3.9 (5.1)	11.1 ± 1	−7
Amundsen subtotal	382,600	150 (151)	222 ± 9	−72 ± 12
A/WHI	235,200	37.5 (32.9)	33.0 ± 1	+5
C	153,400	22.8 (21.7)	0.5 ± 0	+22
D	140,300	20.6 (20.7)	16.7 ± 0	+4
E	175,200	27.9 (23.1)	26.6 ± 1	+1
F	16,800	2.7 (3.0)	1.6 ± 0	+1
Ross subtotal	720,900	111 (101)	78 ± 1	+33 ± 6
EVA	108,400	45.2 (45.7)	50.6 ± 3	−5
CAR	9,100	2.9 (4.0)	2.6 ± 0	+0
RUT	52,600	18.1 (20.6)	17.6 ± 1	+0
INS	166,900	25.5 (30.2)	26.0 ± 2	−1
FOU	221,600	28.0 (26.6)	31.7 ± 3	−4
Weddell subtotal	558,600	120 (127)	128 ± 5	−9 ± 8
West Antarctica total	**1,662,100 (75%)**	**381 (379)**	**429 ± 10**	**−48 ± 14**
BAI	66,700	7.6 (7.5)	7.9 ± 1	−0
SLE	499,200	33.0 (36.7)	31.6 ± 2	+1
REC	964,300	43.8 (52.7)	39.6 ± 3	+4
Weddell subtotal	1,530,200	84 (97)	79 ± 4	+5 ± 6
DAV	214,300	13.7 (19.5)	15.6 ± 1	−2
COO	107,900	20.0 (21.9)	19.8 ± 1	−0
NIN	170,800	25.5 (24.0)	21.9 ± 2	+4
MER	82,600	21.2 (21.2)	19.1 ± 2	+2
TOT	537,900	62.0 (75.6)	69.6 ± 4	−8
DEN	186,300	32.5 (46.4)	31.9 ± 2	+1
SCO	29,500	9.4 (14.2)	9.2 ± 1	+0
LAM	953,700	54.3 (56.0)	57.5 ± 2	−3
RAY	104,000	12.0 (11.0)	11.6 ± 1	+0
SHI	196,700	16.9 (17.1)	15.1 ± 2	+2
JUT	122,500	13.0 (16.7)	13.4 ± 1	−0
STA	99,900	14.8 (17.1)	16.6 ± 2	−2
25°W to 165°E subtotal	2,806,100	295 (341)	301 ± 7	−6 ± 16
BYR	1,070,400	44.7 (60.3)	23.6 ± 2	+21
MUL	115,000	8.2 (7.6)	6.8 ± 1	+1
Ross subtotal	1,185,400	53 (68)	30 ± 2	+23 ± 4
East Antarctica total	**5,521,700 (55%)**	**433 (505)**	**411 ± 8**	**+22 ± 23**

References and Notes

1. J. A. Church *et al.*, in *Changes in Sea Level, IPCC Third Scientific Assessment of Climatic Change*, J. T. Houghton, D. Yihui, Eds. (Cambridge Univ. Press, Cambridge, 2002), chap. 11.
2. R. C. Bales, J. R. McConnell, E. Mosley-Thompson, B. Csatho, *J. Geophys. Res.* **106**, 33183 (2001).
3. M. Giovinetto, J. Zwally, *Ann. Glaciol.* **31**, 171 (2000).
4. D. G. Vaughan, J. L. Bamber, M. Giovinetto, J. Russell, P. R. Cooper, *J. Clim.* **12**, 933 (1999).
5. W. T. Pfeffer, M. F. Meier, T. H. Illangasekare, *J. Geophys. Res.* **96**, 22117 (1991).
6. R. J. Braithwaite, *J. Glaciol.* **41**, 153 (1995).
7. C. Davis *et al.*, *J. Geophys. Res.* **106**, 33743 (2001).
8. D. J. Wingham, A. J. Ridout, R. Scharroo, R. J. Arthern, C. K. Schum, *Science* **282**, 456 (1998).
9. W. Krabill *et al.*, *Science* **289**, 428 (2000).
10. C. R. Bentley, J. M. Wahr, *J. Glaciol.* **44**, 207 (1998).
11. J. Wahr, D. Wingham, C. R. Bentley, *J. Geophys. Res.* **105**, 16279 (2000).
12. R. H. Thomas *et al.*, *J. Geophys. Res.* **106**, 33691 (2001).
13. J. R. McConnell *et al.*, *Nature* **406**, 877 (2000).
14. W. Abdalati *et al.*, *J. Geophys. Res.* **106**, 33729 (2001).
15. R. H. Thomas *et al.*, *J. Geophys. Res.* **106**, 33707 (2001).
16. E. Rignot, S. Gogineni, I. Joughin, W. Krabill, *J. Geophys. Res.* **106**, 34007 (2001).
17. I. Joughin, M. Fahnestock, D. MacAyeal, J. L. Bamber, P. Gogineni, *J. Geophys. Res.* **106**, 34021 (2001).
18. Goddard Institute for Space Studies, Surface Temperature: Station Data (www.giss.nasa.gov/data/update/gistemp/station_data).
19. W. S. B. Paterson, N. Reeh, *Nature* **414**, 60 (2001).
20. M. C. Serreze *et al.*, *Clim. Change* **46**, 159 (2000).
21. R. R. Dickson *et al.*, *J. Clim.* **13**, 2671 (2000).
22. H. J. Zwally *et al.*, *Science* **297**, 218 (2002); published online 6 June 2002 (10.1126/science.1072708).
23. A. Weidick, *Rapp. Gronlands Geol. Unders.* **152**, 73 (1991).
24. C. R. Bentley, M. B. Giovinetto, in *Proceedings of the International Conference on the Role of Polar Regions in Global Change*, G. Weller *et al.*, Eds. (Geophysical Institute, University of Alaska, Fairbanks, AK, 1991), vol. II, pp. 481–486.
25. J. L. Bamber, R. A. Bindschadler, *Ann. Glaciol.* **25**, 439 (1997).
26. M. B. Lythe, D. G. Vaughan, *J. Geophys. Res.* **106**, 11335 (2001).
27. K. C. Jezek, *Ann. Glaciol.* **29**, 286 (1999).
28. A. L. Gray, N. Short, K. E. Mattar, K. C. Jezek, *Can. J. Remote Sens.* **27**, 193 (2001).
29. I. Joughin *et al.*, *Science* **286**, 283 (1999).
30. E. Rignot, *Ann. Glaciol.* **34**, 217 (2002).
31. I. Joughin, S. Tulaczyk, *Science* **295**, 476 (2002).
32. S. Shabtaie, C. R. Bentley, *J. Geophys. Res.* **92**, 1311 (1987).
33. J. H. Mercer, *Nature* **271**, 321 (1978).
34. R. A. Bindschadler, *Science* **282**, 428 (1998).
35. R. B. Alley, R. A. Bindschadler, in *The West Antarctic Ice Sheet, Behavior and Environment*, R. B. Alley, R. A. Bindschadler, Eds. (American Geophysical Union, Washington, DC, 2001), pp. 1–12.
36. E. Rignot, *Science* **281**, 549 (1998).
37. ———, *J. Glaciol.* **47**, 213 (2001).
38. ———, D. G. Vaughan, M. Schmeltz, T. Dupont, D. MacAyeal, *Ann. Glaciol.* **34**, 189 (2002).
39. J. Zwally, personal communication.
40. A. Shepherd, D. J. Wingham, J. A. D. Mansley, H. F. J. Corr, *Science* **291**, 862 (2001).
41. ———, *Geophys. Res. Lett.* **29**, 2-1 (2002).
42. E. Rignot, S. S. Jacobs, *Science* **296**, 2020 (2002).
43. S. S. Jacobs, C. F. Giulivi, P. A. Mele, *Science* **297**, 386 (2002).
44. C. W. M. Swithinbank, in *Satellite Image Atlas of Glaciers of the World, USGS Prof. Pap. 1386-B* (1988).
45. D. G. Vaughan, G. J. Marshall, W. M. Connolley, J. C. King, R. Mulvaney, *Science* **293**, 1777 (2001).
46. C. S. M. Doake, H. F. J. Corr, H. Rott, P. Skvarca, N. W. Young, *Nature* **391**, 778 (1998).
47. T. A. Scambos, C. Hulbe, M. Fahnestock, J. Bohlander, *J. Glaciol.* **46**, 516 (2000).
48. D. G. Vaughan, in *The Contribution of Antarctic Peninsula Ice to Sea Level Rise*, E. M. Morris, Ed. (British Antarctic Survey, Ice and Climate Special Report No. 1, Cambridge, 1992), pp. 35–44.
49. C. Mayer, P. Huybrechts, *J. Glaciol.* **45**, 384(1999).
50. R. B. Alley, I. M. Whillans, *Science* **254**, 959(1991).
51. R. C. A. Hindmarsh, E. Le Meur, *J. Glaciol.* **47**, 271 (2001).
52. R. H. Thomas, *Geogr. Phys. Quat.* **31**, 347 (1977).
53. H. Rott, W. Rack, *Ann. Glaciol.* **34**, 277 (2002).
54. J. L. Bamber, D. G. Vaughan, I. Joughin, *Science* **287**, 1248 (2000).

55. We thank S. Manizade for preparing Fig. 1, J. Zwally for sharing his radar altimetry results in advance of publication, and J. Bamber, I. Joughin, N. Reeh, H. Rott for making their results available for this review. Comments by W. Abdalati, C. R. Bentley, R. Bindschadler, J. Smith, and two anonymous reviewers helped improve the manuscript. E.R. performed this work at the Jet Propulsion Laboratory under a contract with NASA's Cryospheric Science Program. R.H.T. was supported by a contract from the NASA ICESat project.

REVIEW

Air-Snow Interactions and Atmospheric Chemistry

Florent Dominé[1]* and Paul B. Shepson[2]*

The presence of snow greatly perturbs the composition of near-surface polar air, and the higher concentrations of hydroxyl radicals (OH) observed result in a greater oxidative capacity of the lower atmosphere. Emissions of nitrogen oxides, nitrous acid, light aldehydes, acetone, and molecular halogens have also been detected. Photolysis of nitrate ions contained in the snow appears to play an important role in creating these perturbations. OH formed in the snowpack can oxidize organic matter and halide ions in the snow, producing carbonyl compounds and halogens that are released to the atmosphere or incorporated into snow crystals. These reactions modify the composition of the snow, of the interstitial air, and of the overlying atmosphere. Reconstructing the composition of past atmospheres from ice-core analyses may therefore require complex corrections and modeling for reactive species.

Snow can cover up to 50% of landmasses in the Northern Hemisphere (*1*). It forms a porous medium that remains permeable to gases over depths of several meters (*2*). The snowpack—the annually accumulated snow at high latitudes or altitudes—therefore offers a large internal surface for interactions with atmospheric gases.

Evidence for such interactions, and their impact on atmospheric chemistry, was found in the mid-1980s, when it was shown that at high latitudes, ozone could be destroyed completely at altitudes up to 1 km over large areas (*3*). Reactions of halogen species in the snowpack and on aerosol surfaces had to be invoked to explain this observation, which could not be understood on the basis of gas-phase chemistry alone (*4–8*). Similarly, the rapid oxidation of lower atmospheric gas-phase elemental mercury (Hg) to reactive gas-phase and particulate-phase Hg (*9–10*) could only be explained once snowpack and/or sea-ice processes were invoked.

A detailed understanding of snow-atmosphere interactions is necessary for understanding current atmospheric processes, as well as for investigating those of the past using ice cores. In the past few years, extensive measurement campaigns in 2000 in Greenland (at Summit, 73°N) and the Canadian high Arctic (at Alert, 82°N) (Fig. 1) and in Antarctica (at South Pole in 1998–1999, and on the Antarctic coast at Neumayer, 70°S, in 1999) have provided evidence for the impact of the snowpack on many trace atmospheric species. As a result, some insights into the underlying mechanisms are emerging, although the overall picture is still not well understood.

Snowpack Chemistry

Because they control the oxidative capacity of the atmosphere through ozone production (*11*), nitrogen oxides ($NO + NO_2 = NO_x$)

[1]CNRS, Laboratoire de Glaciologie et Géophysique de l'Environnement, B.P. 96, 54 Rue Molière, 38402 Saint Martin d'Hères cedex, France. [2]Department of Chemistry and Department of Earth and Atmospheric Sciences, Purdue University, West Lafayette, IN 47907, USA.

*To whom correspondence should be addressed. E-mail: florent@lgge.obs.ujf-grenoble.fr, pshepson@purdue.edu